

Deconfinement of strangeness and freeze-out from charge fluctuations

Swagato Mukherjee* †

Physics Department, Brookhaven National Laboratory, Upton, NY 11973, USA

E-mail: swagato@bnl.gov

Mathias Wagner

Fakultät für Physik, Universität Bielefeld, D-33615 Bielefeld, Germany

E-mail: mwagner@physik.uni-bielefeld.de

We use Lattice QCD calculations of fluctuations and correlations of various conserved charges to show that the deconfinement of strangeness takes place in the chiral crossover region of QCD; however, inside the quark-gluon plasma strange quarks remain strongly interacting at least up to temperatures twice the QCD crossover temperature. Further, we discuss how the freeze-out parameters of heavy-ion collisions can be determined in a model-independent way through direct comparisons between experimentally measured higher order cumulants of conserved charges and corresponding Lattice QCD calculations. Utilizing the preliminary data from the STAR and PHENIX experiments we illustrate this method. Although, the Lattice QCD based determinations of the freeze-out parameters utilizing data sets of different experiments and different observables are currently not consistent with each other, it is tantalizing to see that all the observed freeze-out parameters lie very close to the chiral/deconfinement crossover region of QCD.

*8th International Workshop on Critical Point and Onset of Deconfinement,
March 11 to 15, 2013
Napa, California, USA*

*Speaker.

†This work has been supported in part through contract DE-AC02-98CH10886 with the U.S. Department of Energy.

1. Introduction

Understanding the nature of strongly interacting matter demands a detailed knowledge regarding the phase structure of Quantum ChromoDynamics (QCD), the underlying theory of strong interaction. Several experimental programs, such as the recent Beam Energy Scan (BES) program at the Relativistic Heavy Ion Collider (RHIC), Brookhaven National Laboratory as well as future experiments at the upcoming FAIR and NICA facilities, have been dedicated to uncover the phase diagram of QCD under extreme conditions, i.e., high temperatures and/or large densities. On the other hand, to complete our knowledge of the QCD phase diagram it is also necessary to supplement these experimental endeavors with first-principle based theoretical calculations. Over the years Lattice QCD (LQCD) has emerged as the most successful technique for performing non-perturbative, parameter free theoretical calculations starting from the QCD Lagrangian.

In this talk we discuss two recent LQCD calculations that closely complement the experimental explorations of the QCD phase diagram. First, we present evidence that at zero baryon density the deconfinement of strangeness takes place in conjunction with the chiral crossover. Next, we describe a method for a model independent determination of the freeze-out temperature and chemical potentials of heavy ion collision experiments through a direct comparisons between the state-of-the-art LQCD calculations and the experimentally measured cumulants of charge fluctuations.

To address these issues we rely on the LQCD computations of the generalized susceptibilities of the conserved charges

$$\chi_{mn}^{XY} = \left. \frac{\partial^{(m+n)} [p(\hat{\mu}_X, \hat{\mu}_Y)/T^4]}{\partial \hat{\mu}_X^m \partial \hat{\mu}_Y^n} \right|_{\vec{\mu}=0}, \quad (1.1)$$

where $\vec{\mu} = (\mu_B, \mu_S, \mu_Q)$ are respectively the baryon number, strangeness and electric charge chemical potentials and $X, Y = B, S, Q$. For brevity, we use the notations $\chi_{0n}^{XY} \equiv \chi_n^Y$ and $\chi_{m0}^{XY} \equiv \chi_m^X$. These generalized susceptibilities are related to the cumulants, such as the mean (M_X), variance (σ_X), skewness (S_X) and kurtosis (κ_X), of the fluctuations of the conserved charge. For example— $VT^3 \chi_1^Q = \langle N_Q \rangle = M_Q$, $VT^3 \chi_2^Q = \langle (\delta N_Q)^2 \rangle = \sigma_Q^2$, $VT^3 \chi_3^Q = \langle (\delta N_Q)^3 \rangle = \sigma_Q^3 S_Q$ and $VT^3 \chi_4^Q = \langle (\delta N_Q)^4 \rangle - 3 \langle (\delta N_Q)^2 \rangle^2 = \sigma_Q^4 \kappa_Q$; V being the volume, T the temperature and N_X the net charge with $\delta N_X = N_X - \langle N_X \rangle$. Details of the LQCD calculations presented here can be found in [1, 2, 3, 4].

2. Deconfinement of strangeness and strange degrees of freedom inside quark gluon plasma

In an uncorrelated gas of hadrons, such as in the Hadron Resonance Gas (HRG) model [5], the dimensionless partial pressure, $P_S \equiv (p - p_{S=0})/T^4$, of the strangeness carrying Degrees of Freedom (sDoF) can be written as

$$P_S^{HRG}(\hat{\mu}_B, \hat{\mu}_S) = P_{|S|=1, M}^{HRG} \cosh(\hat{\mu}_S) + P_{|S|=1, B}^{HRG} \cosh(\hat{\mu}_B - \hat{\mu}_S) \\ + P_{|S|=2, B}^{HRG} \cosh(\hat{\mu}_B - 2\hat{\mu}_S) + P_{|S|=3, B}^{HRG} \cosh(\hat{\mu}_B - 3\hat{\mu}_S), \quad (2.1)$$

where $P_{|S|=1, M}^{HRG}$ is the partial pressure of all $|S| = 1$ mesons and $P_{|S|=i, B}^{HRG}$ are the partial pressures of all $|S| = i$ ($i = 1, 2, 3$) baryons at $\vec{\mu} = 0$. In the above expression the (classical) Boltzmann approximation has been employed for all strange hadrons as their masses are substantially larger

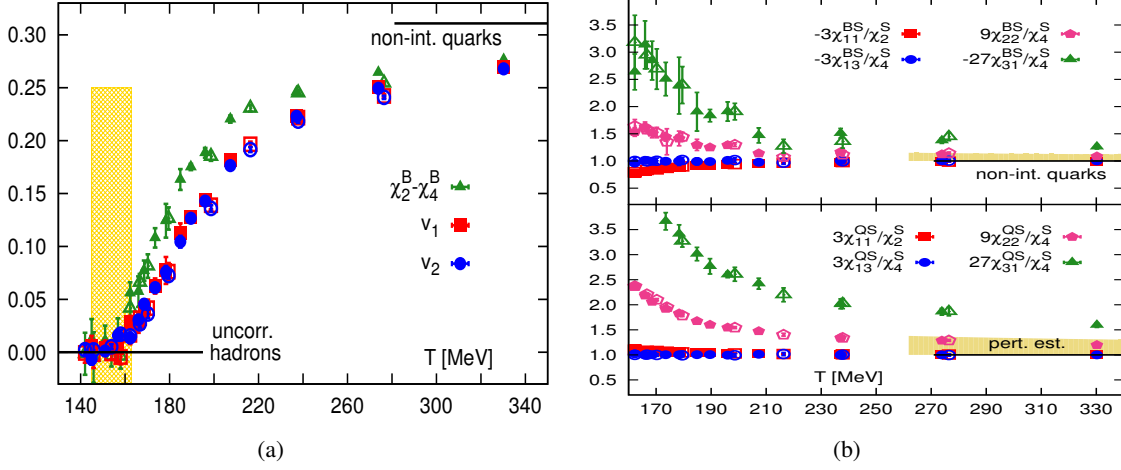


Figure 1: (a) Two combinations, v_1 and v_2 , of strangeness fluctuations and baryon-strangeness correlations that vanish identically if the sDoF are described by an uncorrelated gas of hadrons. The solid lines at low and high temperatures indicate the two limiting scenarios when the dof are described by an uncorrelated hadron gas and non-interacting massless quark gas, respectively. The chiral crossover temperature $T_c = 154(9)$ MeV [4] is indicated by the shaded region. Further shown is the difference of quadratic and quartic baryon number fluctuations, $\chi_2^B - \chi_4^B$, that also vanishes when the baryon number carrying degrees of freedom are strange and non-strange baryons. (b) Baryon-strangeness (top) and electric charge-strangeness correlations (bottom), normalized by the strangeness fluctuations and scaled by appropriate powers of the baryonic and electric charges of a strange quark such that in a non-interacting massless quark gas all these observables are unity (indicated by the lines at high temperatures). The shaded regions indicate the range of perturbative estimates for all these observables obtained using one-loop re-summed Hard Thermal Loop calculations [6]. The open and filled symbols are the LQCD results [1] for two different lattice spacings corresponding to the temporal extents $N_\tau = 6$ and 8, respectively.

than the temperature range of interest. To probe whether the sDoF are associated with integral strangeness and baryon number, as in the case of a hadron gas, we introduce [1] the following combinations consisting of the strangeness fluctuations and baryon-strangeness correlations

$$v_1 = \chi_{31}^{BS} - \chi_{11}^{BS}, \quad \text{and} \quad v_2 = \frac{1}{3} [\chi_2^S - \chi_4^S] - [2\chi_{13}^{BS} - 4\chi_{22}^{BS} - 2\chi_{31}^{BS}]. \quad (2.2)$$

From Eq. (1.1) and Eq. (2.1) it is easy to see that these two combinations vanish exactly for an uncorrelated gas of hadrons, *i.e.* $v_1^{HRG} = v_2^{HRG} = 0$. Since in a hadron gas the sDoF are associated with $|B| = 1$, baryon-strangeness correlations differing by even numbers of μ_B derivatives are identical, leading to $v_1^{HRG} = 0$. On the other hand, the two parenthetically enclosed combinations in the expression of v_2 individually amount to the partial pressure of the $|S| = 2, 3$ baryons, giving $v_2^{HRG} = 0$. The LQCD results [1] for these two combinations are shown in Fig. 1(a). There we also draw the difference between the quadratic (χ_2^B) and the quartic (χ_4^B) baryon number fluctuations that also receive contributions from the light up and down quarks. This combination also vanishes when the strange and light quarks are confined within hadrons following the same argument as for v_1^{HRG} . It is clear that the LQCD data for v_1 , v_2 and $\chi_2^B - \chi_4^B$ are consistent with zero up to chiral crossover temperature $T_c = 154(9)$ MeV [4] and show a rapid increase towards their non-interacting massless quark gas values above the T_c region. The sDoF behave quite similarly as those

involving the light quarks; they are consistent with a hadronic description up to T_c and show rapid departures above T_c . The vanishing values of these observables at low temperatures do not depend on the mass spectrum of the relevant degrees of freedom, as long as they are uncorrelated and the Boltzmann approximation is applicable. It stems from the fact that they carry integer strangeness $|S| = 0, 1, 2, 3$ and baryon number $|B| = 0, 1$. Thus, altogether, LQCD provides strong indications that up to the chiral crossover strangeness remains confined within hadrons and the deconfinement of strangeness takes place around the chiral crossover temperatures.

Based on experimental results from the RHIC and LHC by now it has been generally accepted that for moderately high temperatures the deconfined Quark Gluon Plasma (QGP) phase of QCD remains strongly interacting. It is an intriguing question whether such a strongly interacting QGP consists of quasi-quarks or its is strongly coupled system devoid of a quasi-particle description. To elucidate the nature of sDoF inside the QGP at moderately high temperatures we study the correlations of net strangeness fluctuations with fluctuations of net baryon number and electric charge. For weakly/non-interacting quasi-quarks strangeness $S = -1$ always comes with a baryon number of $B = 1/3$ and an electric charge of $Q = -1/3$. Thus,

$$\frac{\chi_{mn}^{BS}}{\chi_{m+n}^S} = \frac{(-1)^n}{3^m}, \quad \text{and} \quad \frac{\chi_{mn}^{QS}}{\chi_{m+n}^S} = \frac{(-1)^{m+n}}{3^m}, \quad \text{where } m, n > 0, m+n = 2, 4. \quad (2.3)$$

LQCD results [1] for these ratios, scaled by the proper powers of the fractional baryonic and electric charges, are shown in Fig. 1(b). Each of these scaled baryon/charge-strangeness correlations should be unity for a massless gas of non-interacting quasi-quarks. For $T_c \lesssim T \lesssim 2T_c$ the LQCD results for the second order baryon/charge-strangeness correlations are far from the values expected for non-interacting quarks. To illustrate the effects of weak interactions among the quasi-quarks we also indicate (shaded regions at high temperatures) the ranges of values for these ratios as predicted for the weakly interacting quasi-quarks. These values have been calculated from the re-summed Hard Thermal Loop perturbation theory at the one-loop order [6], using one-loop running coupling obtained at the scales between πT and $4\pi T$. LQCD results involving correlations of strangeness with higher power of baryon number and electric charge clearly indicate that a description in terms of weakly interacting quasi-quarks cannot be valid for temperatures $T \lesssim 2T_c$. Thus LQCD results provide unambiguous evidence that sDoF inside QGP can only become compatible with the weakly/non-interacting quasi-quarks only for temperatures $T \gtrsim 2T_c$.

3. LQCD based model independent determination of freeze-out conditions in heavy ion collisions

In Heavy-Ion Collisions (HIC) experiments the measured hadrons come from the freeze-out stage of the fireball evolution. The success of statistical hadronization models [5] in fitting the experimentally measured hadron yields suggests that freeze-out conditions in HIC can be described by equilibrium thermodynamics characterized by freeze-out temperatures (T^f) and chemical potentials ($\mu_B^f, \mu_Q^f, \mu_S^f$). Thus, if at all, the thermal conditions probed in HIC corresponds to these freeze-out parameters. To capture any signature of criticality in HIC the freeze-out must occur close to the QCD crossover/transition in the $T - \mu_B$ plane. By now we have quite reliable knowledge regarding the location of the chiral and deconfinement crossover of QCD in the $T - \mu_B$ plane,

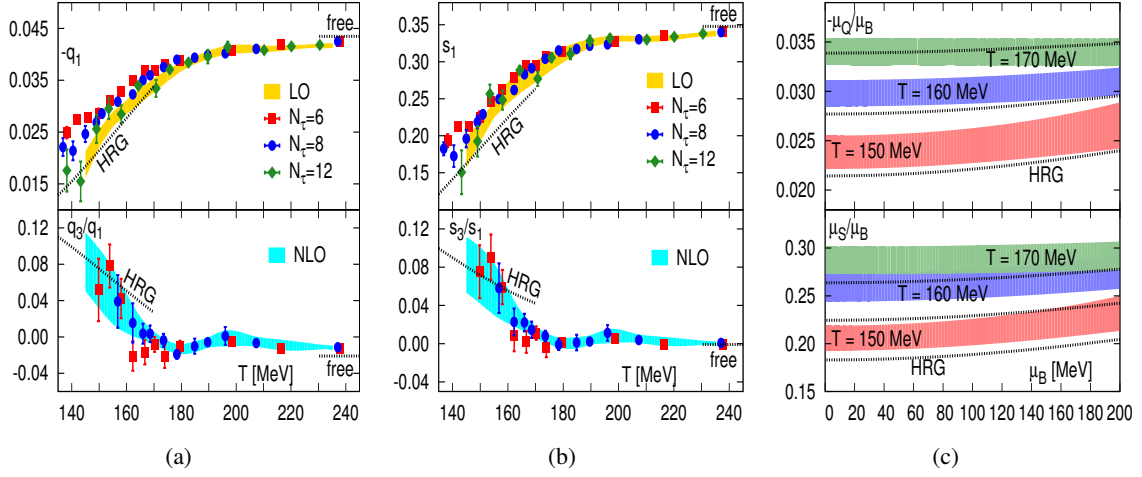


Figure 2: (a) LQCD results [2] for the LO (top) and the NLO (bottom) in μ_B contributions for the electric charge chemical potential as a function of temperature. (b) Same as the previous panel, but for the strangeness chemical potential. (c) Electric charge (top) and strangeness (bottom) chemical potential as a function of μ_B for the relevant temperature range $T = 150 - 170$ MeV.

for moderately small values of μ_B , from first-principle LQCD calculations [1, 4, 7]. On the other hand, so far the freeze-out conditions of HIC have not been determined on an equal footing but only by using model fits [5]. Here we introduce a new methodology for a model independent extraction of the freeze-out parameters through a comparison between experimentally measured cumulants of conserved charge fluctuations and LQCD calculations [2].

For a consistent determination of μ_Q^f and μ_S^f it necessary to realize that these two parameters are not independent of T^f and μ_B^f owing to the initial strangeness neutrality and initial iso-spin asymmetry of the colliding nuclei of HIC. As the net electric charge and net strangeness remain conserved throughout the evolution of the fireball, assuming spatial homogeneity, the initial strangeness neutrality leads to $\langle n_S \rangle = 0$ and the initial iso-spin asymmetry of the colliding nuclei translates into the relation $\langle n_Q \rangle = r \langle n_B \rangle$. Here, n_X denotes the density of the corresponding net conserved charge X and $r = N_p / (N_p + N_n)$ is the ratio of the total number of protons to the total number of protons and neutrons of the initially colliding nuclei. For the RHIC Au-Au and the LHC Pb-Pb collisions $r = 0.4$ provides a good approximation and will be used in our consistent determination for μ_Q^f and μ_S^f . Through a Taylor series expansion of $\langle n_X \rangle$ in powers of (μ_B, μ_Q, μ_S) up to $\mathcal{O}(\mu_X^3)$ and by imposing the above constraints it is possible to write down μ_Q and μ_S in terms of the T^f and μ_B^f [2]

$$\mu_Q(T, \mu_B) = q_1(T)\mu_B + q_3(T)\mu_B^3 + \mathcal{O}(\mu_B^5), \quad \mu_S(T, \mu_B) = s_1(T)\mu_B + s_3(T)\mu_B^3 + \mathcal{O}(\mu_B^5). \quad (3.1)$$

In Fig. 2(a) and Fig. 2(b) we show LQCD results for the Leading Order (LO) contribution $q_1(T)$ and $s_1(T)$ (top panel) and the Next-to-Leading Order (NLO) contribution $q_3(T)$ and $s_3(T)$ (bottom panel) to μ_Q and μ_S , respectively. The NLO contributions are below 10% and are well controlled for a baryon chemical potential $\mu_B \lesssim 200$ MeV, *i.e.* for RHIC energies down to $\sqrt{s_{NN}} \gtrsim 19.6$ GeV. The complete LO plus NLO results for $\mu_Q(T, \mu_B)$ (top panel) and $\mu_S(T, \mu_B)$ (bottom panel) as a function of μ_B for the relevant temperature range $T = 150 - 170$ MeV are shown in Fig. 2(c).

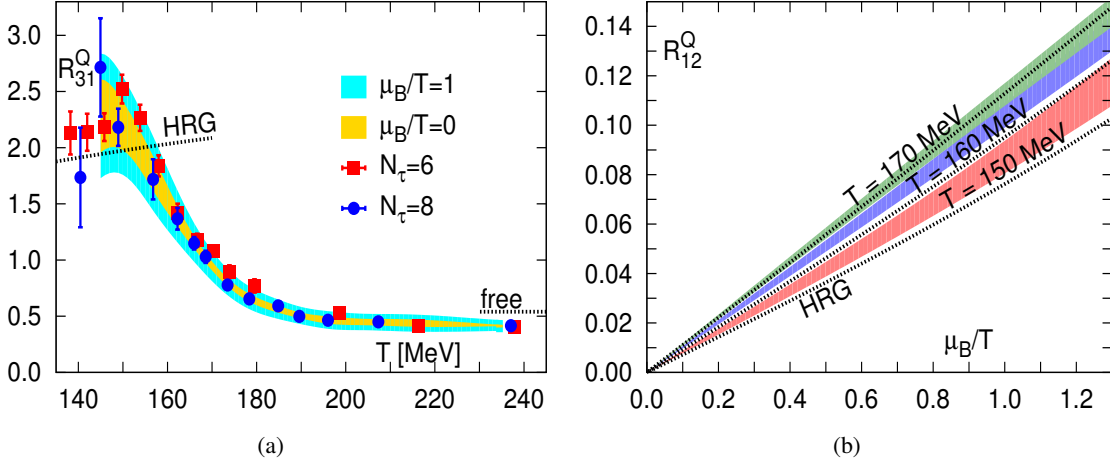


Figure 3: LQCD results [2] for the *thermometer* R_{31}^Q (a) and the *baryometer* R_{12}^Q (b) up to order μ_B^2 .

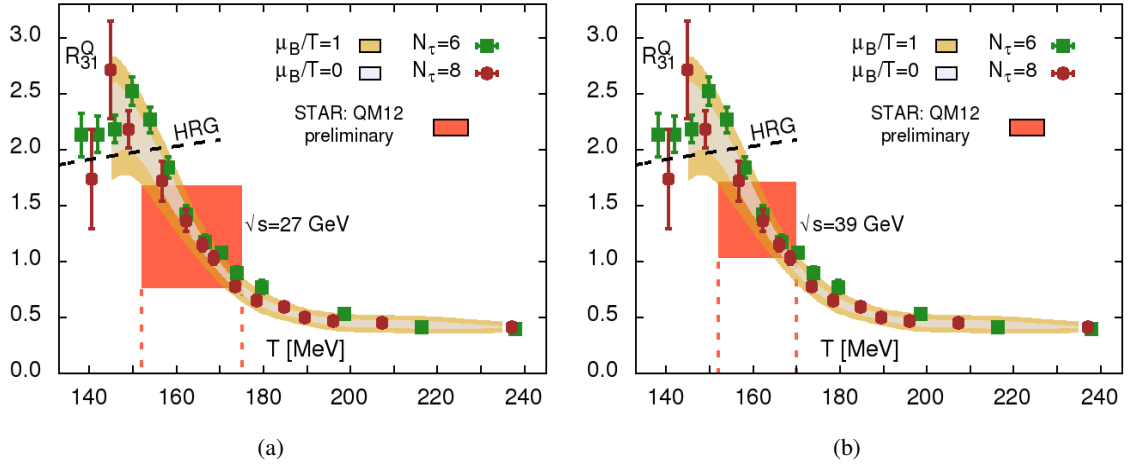


Figure 4: Comparisons between the LQCD results [2] for the *thermometer* R_{31}^Q and the ratio $(S_Q \sigma_Q^3)/M_Q$ of the cumulants of the net electric charge fluctuation measured by the STAR experiment [9] at RHIC beam energies of $\sqrt{s_{NN}} = 27$ GeV (a) and $\sqrt{s_{NN}} = 39$ GeV. The overlap regions of the experimental results with the LQCD calculations provide estimates for the freeze-out temperatures at these energies.

Note that around $T \approx 157$ MeV the LQCD results for $\mu_S/\mu_B \approx 0.24$ is quite close to that extracted from the statistical model based fits of the strange baryons to anti-baryons ratios measures by the STAR experiment as part of the RHIC BES program [8]. This observation not only confirms that strangeness neutrality is also realized during these HIC but also provides a hint for the value of the freeze-out temperature.

To eliminate the explicit (unknown) volume factors we choose to work with the ratios of cumulants of conserved charge fluctuations. As discussed in the Introduction, the experimentally measurable ratios of cumulants are related to the ratios of generalized susceptibilities. With the knowledge of $\mu_Q(T, \mu_B)$ and $\mu_S(T, \mu_B)$ all these susceptibilities can be calculated as function of (T, μ_B) using LQCD with a Taylor series expansion in μ_B . Since the fluctuations of the net electric charge can be measured both in experiments and LQCD, as an explicit example we consider the following

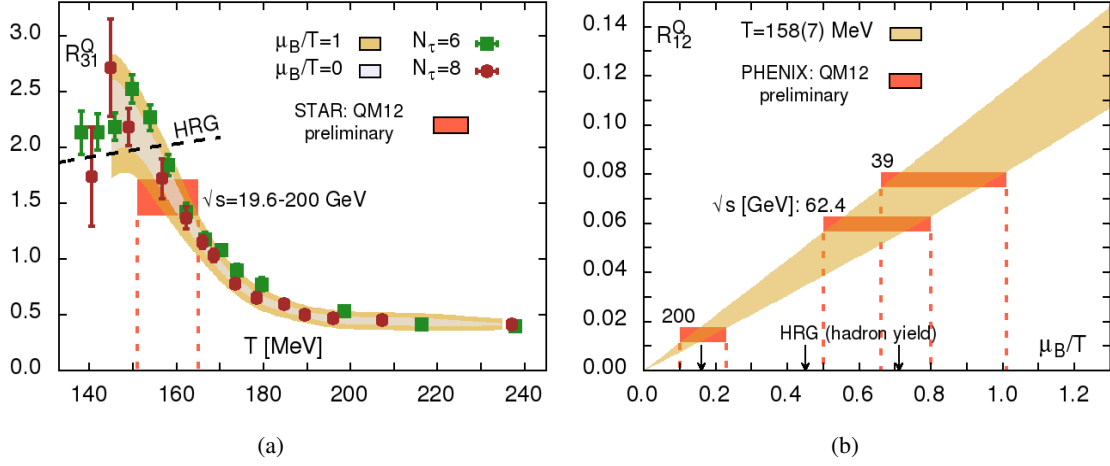


Figure 5: (a) Comparisons between the LQCD results [2] for the *thermometer* R_{31}^Q and the preliminary STAR data [9] for ratio $(S_Q \sigma_Q^3)/M_Q$ of the cumulants of the net electric charge fluctuation, averaged over the energy range $\sqrt{s_{NN}} = 19.6 - 200$ GeV. The overlap of the experimental results with the LQCD calculations provides an estimate for the average freeze-out temperature $T^f = 158(7)$ MeV over $\sqrt{s} = 19.6 - 200$ GeV. (b) LQCD results [2] for the *baryometer* R_{12}^Q as a function of μ_B/T compared with the preliminary PHENIX data [10] for M_Q/σ_Q^2 in the temperature range $T^f = 158(7)$ MeV. The overlap regions of the experimentally measured results with the LQCD calculations provide estimates for the freeze-out chemical potential μ_B^f for a given $\sqrt{s_{NN}}$. The arrows indicate the values of μ_B^f/T^f obtained from traditional statistical model fits to experimentally measured hadron yields [14].

ratios of the cumulants of the net charge fluctuations

$$R_{31}^Q \equiv \frac{\chi_3^Q(T, \mu_B)}{\chi_1^Q(T, \mu_B)} = \frac{S_Q \sigma_Q^3}{M_Q} = R_{31}^{Q,0} + R_{31}^{Q,2} \mu_B^2 + \mathcal{O}(\mu_B^4) \quad (3.2)$$

$$R_{12}^Q \equiv \frac{\chi_1^Q(T, \mu_B)}{\chi_2^Q(T, \mu_B)} = \frac{M_Q}{\sigma_Q^2} = R_{12}^{Q,1} \mu_B + R_{12}^{Q,3} \mu_B^3 + \mathcal{O}(\mu_B^5). \quad (3.3)$$

In LO R_{31}^Q is independent of μ_B while the LO term for R_{12}^Q is proportional to μ_B . This suggests the use of R_{31}^Q as *thermometer* to determine T^f and of R_{12}^Q as *baryometer* to 'measure' μ_B^f . In Fig. 3(a) and Fig. 3(b) we show the LQCD results [2] for the ratio R_{31}^Q and R_{12}^Q , respectively. In the temperature range of interest $T = 150 - 170$ MeV, the estimated NLO corrections for these ratios are below 10% and hence these results are well under control for $\mu_B \lesssim 200$ MeV. Thus, these LQCD data for the *thermometer* R_{31}^Q and the *baryometer* R_{12}^Q can be directly compared with corresponding experimentally measured ratios of net charge cumulants to extract T^f and μ_B^f for RHIC energies down to $\sqrt{s_{NN}} \gtrsim 19.6$ GeV.

As practical demonstrations of this methodology, in Fig. 4(a) and Fig. 4(b) we show comparisons of the LQCD results for the *thermometer* R_{31}^Q with the preliminary STAR data [9] for the corresponding ratio $(S_Q \sigma_Q^3)/M_Q$ of the cumulants of the net charge fluctuation for the RHIC beam energies of $\sqrt{s_{NN}} = 27$ GeV and $\sqrt{s_{NN}} = 39$ GeV, respectively. The freeze-out temperature T^f for a given beam energy can be extracted from the temperature range over which the LQCD calculations and the experimental data overlap. It is clear that the uncertainties of the preliminary

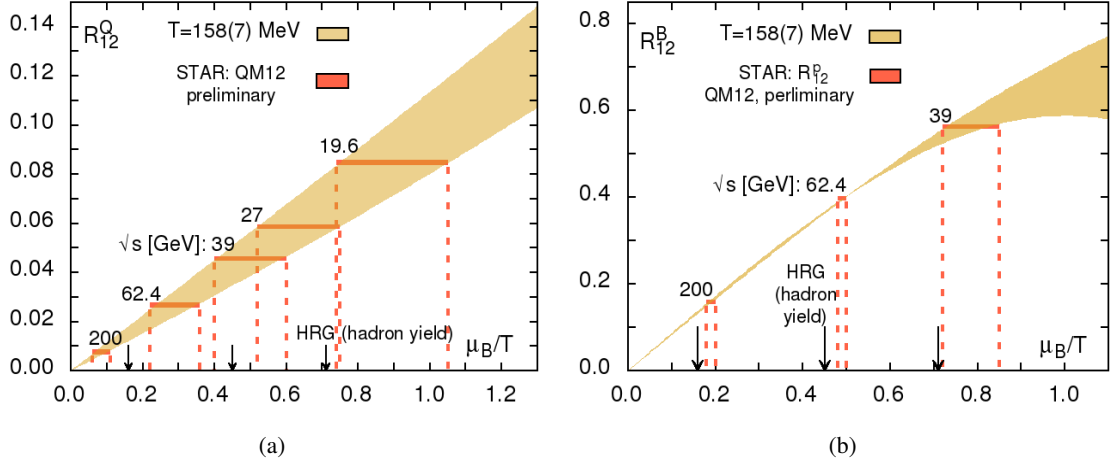


Figure 6: (a) Comparison of the LQCD results [2] for the *baryometer* R_{12}^Q , in the temperature range $T^f = 158(7)$ MeV, with the preliminary STAR data [9] for the ratio M_Q/σ_Q^2 of the cumulants of net charge fluctuation at several RHIC beam energies $\sqrt{s_{NN}}$. (b) LQCD results [2] for the R_{12}^B , in the temperature range $T^f = 158(7)$ MeV, as a function of μ_B/T compared with the preliminary STAR data [13] for the ratio M_p/σ_p^2 of the cumulants of net proton fluctuation. The overlap regions of the experimentally measured and LQCD results provide estimates for the freeze-out chemical potential μ_B^f for a given $\sqrt{s_{NN}}$. The arrows indicate the values of μ_B^f/T^f obtained from traditional statistical model fits to experimentally measured hadron yields [14].

experimental data are too large to extract the $\sqrt{s_{NN}}$ dependence of T^f . Thus, for the illustration of the determination of the μ_B^f we use the preliminary STAR data for $(S_Q\sigma_Q^3)/M_Q$ averaged over the beam energy range $\sqrt{s_{NN}} = 19.6 - 200$ GeV and compare that with the LQCD results of R_{31}^Q in Fig. 5(a). In this way we can determine an average freeze-out temperature of $T^f = 158(7)$ MeV for the RHIC beam energies of $\sqrt{s_{NN}} = 19.6 - 200$ GeV. In this energy range also the traditional statistical model fits [5, 14] yield an almost constant value of T^f . Hence, for the illustrative purpose our use of an average T^f is quite justified. Furthermore, we only use RHIC data for energies down to $\sqrt{s_{NN}} = 19.6$ MeV as for smaller energies μ_B^f becomes too large to justify the use of our LQCD calculations which are performed only up to NLO in μ_B .

In Fig. 5(b) we show the LQCD results for the *baryometer* R_{12}^Q as a function of μ_B/T in the previously determined average freeze-out temperature range of $T^f = 158(7)$ and compare it to the ratio M_Q/σ_Q^2 of the cumulants of the net charge fluctuation measured by the PHENIX collaboration [10] at several RHIC beam energies. Similar comparisons with the preliminary STAR data [9] for M_Q/σ_Q^2 are shown in Fig. 6(a). The freeze-out baryon chemical potential μ_B^f/T^f can be determined from the overlap region of the LQCD and experimental results. Thus, by applying this methodology in a similar manner for each beam energy the corresponding freeze-out temperature and baryon chemical potential can be obtained in a completely model independent way through direct comparisons of the LQCD and HIC experiments.

If the freeze-out stage of HIC is indeed described by equilibrium thermodynamics then thermodynamic consistency demands that T^f and μ_B^f determined through different observables should produce the same values for these thermodynamic parameters. For example, instead of the net electric

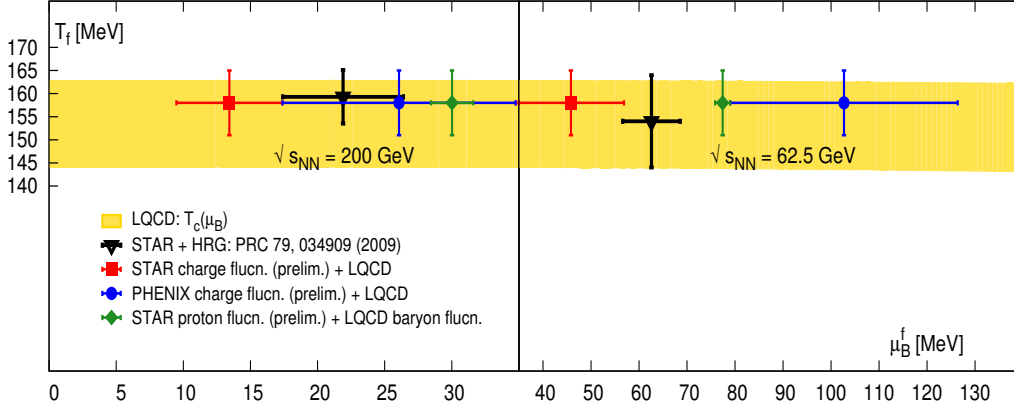


Figure 7: Freeze-out temperatures T^f and baryon chemical potentials μ_B^f obtained through direct comparisons between LQCD calculations and the preliminary STAR and PHENIX data for cumulants of net charge and net proton fluctuations. The shaded region indicate the LQCD results [1, 4, 7] for the chiral/deconfinement temperature T_c as a function of the baryon chemical potential.

charge one may use the fluctuation of net baryon number and use LQCD results for $R_{12}^B = \chi_1^B / \chi_2^B$ as the *baryometer*. Despite the caveat that cumulants of net proton fluctuation may be quantitatively different from the cumulants of net baryon number fluctuation [11, 12], in Fig. 6(b) we present a comparison between the LQCD results for R_{12}^B and the preliminary STAR data [13] for the ratio M_p / σ_p^2 of the cumulants of net proton fluctuation. Unfortunately, as can be seen from Fig. 5(b) and Fig. 6, the freeze-out baryon chemical potential obtained from all these experimental measurements are not consistent with each other at present. Furthermore, they are also not consistent with the freeze-out baryon chemical potential obtained from the traditional statistical model fits to the experimentally measured hadron yields [14]. To illustrate this more clearly in Fig. 7 we show the freeze-out parameters T^f and μ_B^f extracted by comparing LQCD calculations with the preliminary STAR and PHENIX results for the cumulants of net charge fluctuations as well as with the preliminary STAR data for the cumulants of net proton fluctuations. While these results differ from each other and from that obtained using the statistical model fits to the experimentally measured hadron yields [15], it is tantalizing to see that all these results lie within the chiral/deconfinement crossover region, $T_c(\mu_B) = (154(9) - [0.0066(7)/154(9)]\mu_B^2)$ MeV, obtained from LQCD calculations [1, 4, 7]. This makes us hopeful that the HIC collision experiments may signal presence of criticality in the QCD phase diagram in the $T - \mu_B$ plane.

While such direct comparisons between the LQCD calculations and HIC experiments may open up many new opportunities, at present, one has to be somewhat cautious. The LQCD calculations of generalized susceptibilities are performed using a grand-canonical ensemble approach in the thermodynamic limit. It is a-priori not evident that this is also applicable to conditions met in a heavy ion collision. Thus while comparing our results with experimental ones we must make sure that effects of conservation laws due to finite system sizes, acceptance cuts [11, 16] etc. do not invalidate the grand canonical ensemble approach. These questions are currently being addressed in experimental analysis [9, 10, 13] and hopefully will be resolved soon.

References

- [1] A. Bazavov *et al.*, arXiv:1304.7220 [hep-lat].
- [2] A. Bazavov *et al.*, Phys. Rev. Lett. **109**, 192302 (2012).
- [3] A. Bazavov *et al.*, Phys. Rev. D **86**, 034509 (2012).
- [4] A. Bazavov *et al.*, Phys. Rev. D **85**, 054503 (2012).
- [5] For a review see: P. Braun-Munzinger, K. Redlich, and J. Stachel, In *Hwa, R.C. (ed.) et al.: Quark gluon plasma* 491-599, [nucl-th/0304013].
- [6] J. O. Andersen, S. Mogliacci, N. Su and A. Vuorinen, Phys. Rev. D **87**, 074003 (2013).
- [7] O. Kaczmarek *et al.*, Phys. Rev. D **83**, 014504 (2011).
- [8] F. Zhao, this proceedings.
- [9] D. McDonald [STAR Collaboration], Nucl. Phys. A904-905 **2013**, 907c (2013).
- [10] J. T. Mitchell [PHENIX Collaboration], Nucl. Phys. A904-905 **2013**, 903c (2013).
- [11] A. Bzdak and V. Koch, Phys. Rev. C **86**, 044904 (2012).
- [12] M. Kitazawa and M. Asakawa, Phys. Rev. C **85**, 021901 (2012); Phys. Rev. C **86**, 024904 (2012) [Erratum-ibid. C **86**, 069902 (2012)].
- [13] X. Luo [STAR Collaboration], Nucl. Phys. A904-905 **2013**, 911c (2013).
- [14] J. Cleymans, H. Oeschler, K. Redlich and S. Wheaton, Phys. Rev. C **73**, 034905 (2006).
- [15] B. I. Abelev *et al.* [STAR Collaboration], Phys. Rev. C **79**, 034909 (2009)
- [16] A. Bzdak, V. Koch and V. Skokov, Phys. Rev. C **87**, 014901 (2013).